Effects of groundwater table position and soil properties on stability of slope during rainfall

Rahardjo, Harianto; Satyanaga, Alfrendo; Leong, Eng Choon; Ng, Yew Song

2010

Rahardjo, H., Satyanaga, A., Leong, E. C., & Ng, Y. S. (2010). Effects of Groundwater Table Position and Soil Properties on Stability of Slope during Rainfall. Journal of Geotechnical and Geoenvironmental Engineering, ASCE, 136(11), 1555-1564.

https://hdl.handle.net/10356/79885

https://doi.org/10.1061/(ASCE)GT.1943-5606.0000385

Effects of groundwater table position and soil properties on stability of slope during rainfall

Harianto Rahardjo[1]; Alfrendo Satyanaga Nio[1]; Eng Choon Leong[1]; and Ng Yew Song[2]

[1] *School of Civil and Environmental Engineering, Nanyang Technological University, Singapore*
[2] *Building Technology Department, Housing and Development Board, Singapore*

Corresponding author:

Dr. Harianto Rahardjo
Professor and Head of Division
School of Civil & Environmental Engineering
Nanyang Technological University
Blk N1, #1B-36, Nanyang Avenue
Singapore 639798

Phone : +(65) 6790-5246
Fax : +(65) 6791-0676
Email : chrahardjo@ntu.edu.sg
Website : http://www.ntu.edu.sg/cee/

Address of Authors:

Dr. Harianto Rahardjo
Professor and Head of Division
School of Civil & Environmental Engineering
Nanyang Technological University
Blk N1, #1B-36, Nanyang Avenue
Singapore 639798

Phone : +(65) 6790-5246
Fax : +(65) 6791-0676
Email : chrahardjo@ntu.edu.sg
Website : http://www.ntu.edu.sg/cee/

Alfrendo Satyanaga Nio
Project Officer
School of Civil & Environmental Engineering
Nanyang Technological University
Singapore 639798

Phone : +(65) 6790-6814
Fax : +(65) 6791-0676
Email : alfrendo@ntu.edu.sg

Dr. Leong Eng Choon
Associate Professor
School of Civil & Environmental Engineering
Nanyang Technological University
Blk N1, #1C-80, Nanyang Avenue
Singapore 639798

Phone : +(65) 6790-4774
Fax : +(65) 6791-0676
Email : cecleong@ntu.edu.sg

Er. Ng Yew Song
Deputy Director and Professional Engineer
Building Technology Department
Housing & Development Board
HDB Hub 480, Lorong 6, Toa Payoh
Singapore 310480

Phone : +(65) 6490-2502
Fax : +(65) 6490-2501
Email : nys1@hdb.gov.sg

Effects of groundwater table position and soil properties on stability of slope during rainfall

Harianto Rahardjo[1]; Alfrendo Satyanaga Nio[1]; Eng Choon Leong[1]; and Ng Yew Song[2]

ABSTRACT: Rainfall, hydrological condition, and geological formation of slope are important contributing factors to slope failures. Parametric studies were carried out to study the effect of groundwater table position, rainfall intensities and soil properties in affecting slope stability. Three different groundwater table positions corresponding to the wettest, typical and driest period in Singapore and four different rainfall intensities (9 mm/hr, 22 mm/hr, 36 mm/hr and 80 mm/hr) were used in the numerical analyses. Typical soil properties of two main residual soils from the Bukit Timah Granite and the Sedimentary Jurong Formation in Singapore were incorporated into the numerical analyses. The changes in factor of safety during rainfall were not affected significantly by the groundwater table near the ground surface due to the relatively small changes in matric suction during rainfall. A delay in response of the minimum factor of safety due to rainfall and a slower recovery rate after rainfall were observed in slopes from the sedimentary Jurong Formation as compared to those slopes from the Bukit Timah Granite. Numerical analyses of an actual residual soil slope from the Bukit Timah Granite at Marsiling Road and a residual soil slope from the sedimentary Jurong Formation at Jalan Kukoh show good agreement with the trends observed in the parametric studies.

[1] Professor, School of Civil and Environmental Engineering, Nanyang Technological University, Blk N1, #1B-36, Nanyang Avenue, Singapore 639798

[2] Project Officer, School of Civil and Environmental Engineering, Nanyang Technological University, Blk N1, #B4C-10, Nanyang Avenue, Singapore 639798

[3] Associate Professor, School of Civil and Environmental Engineering, Nanyang Technological University, Blk N1, #1C-80, Nanyang Avenue, Singapore 639798

[4] Deputy Director and Professional Engineer, Building Technology Department, Housing & Development Board, HDB Hub 480, Lorong 6, Toa Payoh, Singapore 310480

KEYWORDS: Rainfall intensity; Groundwater table; Residual soils; Matric suction; Permeability; Shear strength; and Slope stability.

1 INTRODUCTION

Many slope failures around the world, particularly in regions with residual soils, occurred due to changes in unsaturated soil condition as a result of frequent heavy rainfalls. Matric suction or negative pore-water pressure plays an important role in the stability of these slopes (Fredlund and Rahardjo, 1993). A deep groundwater table and a significant thickness of unsaturated zone above the groundwater table are general characteristics of steep residual soil slopes. In tropical and subtropical areas, rainfall-induced slope failures are closely related to the properties of the soil, the geometry of the slope, the position of groundwater table and certain environmental factors (vegetation and weathering effects).

Previous research works have shown that rainfall is the main contributing factor of slope failures in Singapore (Brand, 1984; Tan et al., 1987; Chatterjea, 1989; Lim et al., 1996; Toll et al., 1999, Rahardjo et al., 2007). The last heavy rainfall between December 2006 and January 2007 caused a number of slope failures in Singapore. Almost all of slope failures occurred in residual soils from the Bukit Timah Granite and the sedimentary Jurong Formation (Rahardjo et al., 2007).

Numerical analyses of rainfall-induced slope failures have been carried out to study the controlling parameters (Gasmo et al., 2000, Tsaparas et al., 2002, Rahardjo et al., 2005 Rahardjo et al., 2007) and the effects of antecedent rainfall on rainfall-induced slope failures (Rahardjo et al., 2001, Rahardjo et al., 2008). Cho and Lee (2002) indicated that most shallow slope failures were caused by the advancement of a wetting front into slope. Ng et al. (2001) conducted three-dimensional numerical analyses of groundwater response to rainfall and found that rainfall pattern, duration and its return period have major influences on the changes in pore-water pressures in unsaturated cut slopes. Tohari et al. (2007) conducted a laboratory study of slopes under rainfalls and observed that shallow noncircular slip was the dominant mode for rainfall-induced slope failures.

In this paper, parametric studies were performed to study the effect of position of groundwater table, rainfall intensity and soil properties on the stability of slope. The observation was focused on the residual soils from the Bukit Timah Granite and the Sedimentary Jurong Formation in Singapore. Numerical analyses of existing slopes were compared with the results from the parametric studies.

2 SLOPE OBSERVATION

Two thirds of Singapore consist of two major formations, the Bukit Timah Granite and the sedimentary Jurong Formation (PWD, 1976). Bukit Timah Granite underlies the Bukit Timah nature reserve and the central catchment area in the centre of the island. Sedimentary rocks of the Jurong Formation which contain variations of conglomerate, shale and sandstone are located in southern, southwestern and western part of Singapore. Climatic conditions in Singapore are characterized by uniform temperature, high humidity and particularly, abundant rainfalls. The rainy season can be divided into two main seasons, the wetter Northeast Monsoon season from December to March and the drier Southwest Monsoon season from June to September (National Environment Agency, 2007). During the Northeast Monsoon season, moderate to heavy rainfalls usually occur between December and January. Maximum rainfall usually occurs between December and January, whereas July is noted as the driest month (National Environment Agency, 2007).

Several slopes located at the residual soil slopes from the Bukit Timah Granite (BT) and the sedimentary Jurong Formation (JF) were investigated to obtain information on typical soil properties, slope geometry and position of groundwater table for both formations. The investigated slopes had a slope angle and a slope height varying from 15˚ to 40˚ and from 5 to 42 m, respectively.

2.1 Location and Geometry of Slopes

Six slopes were selected from two different geological formations in Singapore. Ang Mo Kio St. 21 (AMK), Thomson Road (TR), and Marsiling Road (MR) slopes are located in the BT, while Bukit Merah View (BM), Jalan Kukoh (JK), and Havelock Road (HR) slopes

are located in the JF (Figure 1). Soil sampling was performed using continuous foam drilling with a Mazier sampler to obtain good quality samples. Laboratory tests were then carried out to obtain saturated and unsaturated hydraulic properties and shear strength of the investigated soils. Soil profiles of the observed slopes could then be constructed. The unsaturated laboratory tests included soil-water characteristic curve (SWCC) tests and unsaturated triaxial tests for obtaining unsaturated shear strength parameters.

2.2 Positions of Groundwater Table

The investigated slopes were instrumented with at least two piezometers to monitor the position of groundwater table. Manual monitoring of the Casagrande piezometers for all slopes was carried out over a two years period (June 2006 until September 2008). Variations of groundwater table positions for the driest and wettest periods are shown in Figures 2 and 3 in the residual soil slopes from BT and JF, respectively. The average positions of groundwater table, representing its typical position in residual soil slopes in Singapore, were calculated based on the minimum position of groundwater table during the dry period and the maximum position of groundwater table during the wet period (Figures 2 and 3). The symbol ℓ in Figures 2 and 3 represents the distance of the piezometers (P1 and P2) measured from the crest of slope, while the symbol h corresponds to the depth of groundwater table from the slope surfaces. Slope vertical heights and slope horizontal lengths were denoted as H and L, respectively.

Figures 2 and 3 show that the groundwater table of the JF slope was generally deeper than that of the BT slope during dry and wet periods. However, the groundwater table of the JF slope indicated a larger difference between dry and wet periods as compared to that of the BT slope. This condition may be attributed to the large variability of soil types in the JF residual soil that was derived from the sedimentary rocks of different variations from conglomerate to shale, siltstone and sandstone. On the other hand, the BT residual soil was derived mainly from the same granitic rock of Bukit Timah formation.

3 SOIL PROPERTIES OF INVESTIGATED SLOPES

3.1 Soil-Water Characteristic Curves

SWCC tests were performed using Tempe cell and pressure plate. Matric suction up to 500 kPa were applied to several specimens of the BT and the JF residual soils taken from various depths. The SWCC of the investigated soils were plotted in terms of normalized volumetric water content, Θ_w, versus matric suction, u_a-u_w. The normalized volumetric water content can be defined with respect to the residual water content of the soil as shown in Equation 1.

$$\Theta_W = \frac{\theta_w - \theta_r}{\theta_s - \theta_r} \quad (1)$$

where Θ_w is the normalized volumetric water content, θ_w is the volumetric water content at particular matric suction, θ_r is the residual volumetric water content and θ_s is the saturated volumetric water content.

The SWCC from two soil layers of Ang Mo Kio (AMK1 and AMK2), two soil layers of Thomson Road (TR1 and TR2), and one soil layer of Marsiling Road (MR1) slopes were collated with the SWCC data of the BT residual soils of Agus et al. (2001). The normalized SWCC data of the BT residual soils are shown in Figure 4.

The SWCC from three soil layers of Bukit Merah View (B1, B2, and B3), two soil layers of Jalan Kukoh (JK1 and JK2), and one soil layer of Havelock Road (HR) slopes were collated with SWCC data of the JF residual soils of Agus et al. (2001). The normalized SWCC data for the JF residual soils were compiled as shown in Figure 5.

The following SWCC equation (Fredlund and Xing, 1994) was used to best fit the data:

$$\theta_W = C(\psi)\frac{\theta_S}{\left\{\ln\left[e + \left(\frac{u_a - u_w}{a}\right)^n\right]\right\}^m} \quad (2)$$

where $C(\psi)$ is correction factor, (u_a-u_w) is matric suction (kPa), e is natural number (2.71828…). The fitting parameter a, n, and m are related to air-entry value of the soil (kPa), the slope of the SWCC, and the residual water content, respectively. Leong and Rahardjo

(1997) suggested using a correction factor of 1. The upper and lower bounds of the normalized SWCC together with typical SWCC for each formation were subsequently drawn on the graphs based on Equation 2 with $C(\psi) = 1$. Typical SWCC was obtained by taking a mean value of volumetric water content for each matric suction within the upper bound and lower bound of SWCC. Then, the mean value of volumetric water content was fitted using Fredlund and Xing equation (Fredlund and Xing, 1994) with correction factor = 1 as suggested by Leong and Rahardjo (Leong and Rahardjo, 1997).

Figure 4 illustrates that the upper and lower bounds of normalized SWCC for the BT residual soils were considered to be the same with those envelopes proposed by Agus et al. (2001). The upper bound of normalized SWCC envelope gave a = 159 kPa, n = 0.93, and m = 1.004 and the lower bound of normalized SWCC envelope gave a = 32 kPa, n = 0.525, and m = 2.243. The typical normalized SWCC fitting parameters were a = 20 kPa, n = 0.8, and m = 0.75.

Figure 5 shows the lower bound of normalized SWCC for the JF residual soils (a = 150 kPa, n = 0.85, and m = 7.5) was lower and steeper than that proposed by Agus et el. (2001). Meanwhile, the upper bound of normalized SWCC (a = 1950 kPa, n = 0.65, and m = 2.25) was observed to be higher than that proposed by Agus et al. (2001). The typical normalized SWCC fitting parameters were a = 1853 kPa, n = 0.56, and m = 5.5. In general, the new envelope of normalized SWCC for the JF soils was wider than that proposed by Agus et al. (2001).

Using the saturated volumetric water content of each soil, the corresponding typical SWCC was then used as the input soil properties in the parametric study, for both BT and JF residual soils (Figures 6 and 7), respectively. It can be observed that the SWCC of the BT residual soils has higher saturated volumetric water content, lower air-entry value, steeper slope, and lower residual water content than those of the JF residual soils.

3.2 Permeability Function

Field and laboratory permeability tests were conducted to obtain saturated permeability, k_s, of the selected residual soils. Saturated permeabilities of the BT and the JF residual soils

were then used in the parametric studies. Permeability functions of the investigated soils were determined indirectly from SWCC using the statistical model (Marshall, 1958; Millington and Quirk, 1959; Kunze et. al., 1968) as explained in Fredlund and Rahardjo (1993). Permeability function of the BT residual soils with $k_s = 3x10^{-5}$ m/s and the JF residual soils with $k_s = 4x10^{-6}$ m/s are shown in Figure 8.

3.3 Shear Strength

Shear strengths of the BT and the JF residual soils were obtained from two types of triaxial tests. The consolidated undrained (CU) triaxial tests with pore-water pressure measurement were carried out to obtain effective cohesion (c') and effective angle of internal friction (ϕ') of the residual soils. Meanwhile, multistage consolidated drained (CD) triaxial tests were performed using a modified triaxial apparatus to obtain an angle indicating the rate of change in shear strength relative to a change in matric suction (ϕ^b) of the residual soils. Typical shear strengths of the observed residual soils were then used in parametric studies. The shear strength parameters of the BT residual soil used in the parametric studies were c' = 3.5 kPa, ϕ' = 31.5º, and ϕ^b = 22.5º. Those values were within the ranges suggested by Leong et al. (2000), i.e. c' = 0~14 kPa, ϕ' = 29º ~32º, and ϕ^b = 15º~32º. The JF soil has c' = 6.5 kPa, ϕ' = 30.5º, and ϕ^b = 22º. Leong et al. (2000) suggested the ranges for c', ϕ', and ϕ^b for the JF residual soil as 5~9 kPa, 27º~35º, and 23º ~35º, respectively.

4 NUMERICAL MODELING OF RESIDUAL SOIL SLOPES IN SINGAPORE

Parametric studies were conducted to assess the stability of residual soil slopes subjected to several independent variables. The controlling independent variables are the position of initial groundwater table, soil properties, and rainfall intensity.

4.1 Controlling Parameters in Numerical Analyses

The study of the effect of groundwater table on the stability of the BT and the JF slopes in Singapore involves six series of parametric studies. Two series were conducted using the initial positions of groundwater table during dry period. The other two series were performed

using the initial positions of groundwater table during wet period. The remaining series of these parametric studies were conducted using the average groundwater table positions of residual soil slopes in Singapore as the initial positions of groundwater table. Based on the Code of Practice of Power and Utilities Board, Singapore (PUB, 1992) for drainage system design, the maximum total amount of rainfall in a day is 533.2 mm. Therefore, a rainfall intensity of 22 mm/hr for a duration of 24 hours was applied in all series of these parametric studies.

A typical slope geometry with height (H) of 15 m, angle of 27˚ and length (L) of 29.4 m (Rahardjo et al., 2000) was used in the model for parametric study of residual soil slopes from the Bukit Timah Granite and the sedimentary Jurong Formation. The initial position of groundwater table for each series of parametric studies was calculated from Figures 2 and 3. As an example, Figure 2 shows that at the wettest period, the groundwater table position in the BT slope was at h/H of 0.653 at the crest (ℓ/L = 0) and at h/H of 0.053 at the toe (ℓ/L = 1) of the slope. In other words, the actual depth of groundwater table (h) was 9.8 m and 0.8 m at the crest and the toe of the BT slope, respectively, corresponding to H = 15m. Similarly, the initial position of groundwater table for the JF slope was calculated from Figure 3 for the wettest and driest periods.

The study of the effect of rainfall intensity on the stability of the BT and the JF slopes in Singapore involved eight series of parametric studies. All series in these parametric studies were conducted using the average groundwater table positions of residual soil slopes in Singapore as the initial positions of groundwater table. Four different rainfall intensities, 9 mm/hr, 22 mm/hr, 36 mm/hr and 80 mm/hr were used in these studies. Paulhus (1965) observed the greatest rainfall intensity in the world is 80 mm/hr. Therefore, this rainfall intensity was also adopted in the numerical analyses. All numerical analyses were conducted for a period of 48 hours with rainfall being applied during the first 24 hours.

4.2 Seepage and Slope Stability Modeling

Two-dimensional seepage analyses were performed in this study using the finite element software, SEEP /W (Geoslope International Pte. Ltd., 2004a). In Singapore, majority

of slope failures occurred within a shallow depth. Simplified slope profiles with a homogeneous soil layer (one layer) from the JF and the BT slope were used in the parametric study. Typical SWCC (Figures 6 and 7) and permeability functions (Figure 8) were used in the numerical analyses.

Boundary conditions were applied to the slope model for the transient seepage analyses. Non-ponding boundary condition was applied in order to prevent excessive accumulation of rainfall on the slope surface. The flux boundary, q, equal to the desired rainfall intensity and duration was applied to the surface of the slope. The nodal flux, Q, equal to zero was applied along the sides above the water table line and along the bottom of the slope in order to simulate no flow zone. The sides below the water table were defined as head boundaries equal to the specific position of the groundwater level (total head, h_w). Initial condition for the slope model was taken as hydrostatic pore-water pressure condition with a limiting negative pore-water pressure of 75 kPa. The limit was imposed to prevent the generation of unrealistic pore-water pressures. Rahardjo et al. (2000) observed that the highest matric suction measured in a few sites in Singapore was 75 kPa. Figure 9 shows the typical slope model and the applied flux boundary conditions. The distance between the slope and the side of the slope model was set to three times the height of the slope to avoid the influence of the side boundary conditions. The finite element model down to 5 m below the slope surface had a mesh size of approximately 0.5 m, smaller than other part of the slope, in order to obtain accurate results within the infiltration zone.

The selected time increment was related to a period of rainfall of 24 hrs. Finer time increments provide more accurate seepage and slope stability analyses. Therefore, the time increments were set as 1, 2, 5, 10, 20, 30 and 60 minutes. The time increment was altered every 10 steps and the total simulated duration was 48 hrs. The pore-water pressures were calculated in Seep/W for every time step at each node of the finite element mesh. The pore-water pressure output of the seepage analyses was incorporated into slope stability analyses.

Slope stability analyses of the BT and the JF slopes were performed using SLOPE/W (Geoslope International Ltd., 2004b). The finite element mesh of the slope model in Seep/W

was imported to Slope/W. The typical saturated and unsaturated shear strengths for the BT and the JF residual soils were used in the slope stability analyses using Bishop's simplified method. The pore-water pressure distribution was selected for each time increment and the corresponding factor of safety was calculated.

4.3 Parametric Studies with Variation of Groundwater Table Position

Variations in factor of safety due to initial groundwater table positions at the BT and the JF residual soil slopes are given in Figures 10 and 11, respectively. Figure 10 shows the factor of safety of the BT slope reached a minimum value when rainfall stopped regardless the position of groundwater table. Factor of safety for the BT slope in the driest period (2.16) and at the average condition (2.04) decreased drastically and reached a minimum value at 1.7. After the rainfall ceased, the factor of safety for the BT slope at the driest period and at the average condition increased rapidly at the same recovery rate. The factor of safety for the BT slope in the wettest period decreased gradually from 1.7 to 1.45 and then it increased slowly after the rainfall stopped.

Figure 11 shows the factor of safety decreased rapidly during the driest period due to the high matric suction of the soil above groundwater table before rainfall. In the wettest period, the decrease in factor of safety was slower as compared to other periods. The factor of safety (2.5) of the JF slope in the driest period decreased significantly to a minimum factor of safety of 1.8 one hour after the rainfall stopped. After which, the factor of safety recovered slowly. The factor of safety (2.0) of the JF slope at the average condition decreased rapidly and reached a minimum factor of safety of 1.6 one hour after the rainfall stopped. Subsequently, it recovered at the same rate as that for the driest period. The factor of safety (1.56) of the JF slope at the wettest period decreased slowly and it reached a minimum value of 1.4 at 12 hours after rainfall stopped.

The groundwater table position affected the initial factor of safety. The closer the groundwater table position to the ground surface, the lower the initial factor of safety would be. The significant difference in the decreasing rate of factor of safety for the JF slope during the driest, average and wettest periods was caused by the wide range of groundwater table

position in the JF slope for those periods. In the driest period, the initial matric suction before rainfall is higher than that in other periods. When rainwater infiltrated into the soil layer, the matric suction decreased drastically, resulting in the significant decrease of factor of safety during dry periods. The minimum factor of safety for the JF slope was not observed at the end of rainfall, but 1 hour after the rainfall stopped for the average groundwater table condition and during the driest period. In the wettest period, the minimum factor of safety was observed 12 hours after the rainfall stopped. However, the time delay to reach the minimum factor of safety was not observed in the BT slope. This could be attributed to the effects of SWCC and permeability function on the JF residual soil. The JF residual soil slope had lower water-entry value and gentler permeability function, resulting in a slower infiltration rate of rainwater than that in the BT slope. Although rainfall already stopped, the rainwater continued to percolate down into greater depths. As a result, the most critical slip surface might be observed several hours after the rainfall stopped.

4.4 Parametric Studies with Variation of Rainfall Intensity

The effects of different rainfall intensities on the stability of the BT and the JF slopes are shown in Figures 12 and 13, respectively. Factor of safety of the BT slope with a rainfall intensity higher than 22 mm/hr decreased drastically during the rainfall period and recovered rapidly after the rainfall stopped. The magnitude and the rate of decrease in factor of safety were related to the rainfall intensity. A higher intensity of rainfall caused the factor of safety to decrease more rapidly. However, the minimum factors of safety for the BT slope with 22, 36, and 80 mm/hr of rainfall intensity were approximately similar. This behavior indicated that the slope had reached its threshold rainfall intensity at 22 mm/hr, beyond which rainfall intensity did not appear to affect the minimum factor of safety significantly because the soil had reached its capacity to receive rainwater. On the other hand, a rainfall intensity of 9 mm/hr (2.5×10^{-6} m/s) had no significant effect on the factor of safety of the BT slope. Figure 8 shows that the BT slope had a low permeability at a high suction. The deep groundwater table of the BT slope created a high matric suction in the BT slope before rainfall, resulting in a low permeability. The application of 9 mm/hr of rainfall for 24 hours was not high enough

to change the matric suction of the BT soil significantly. Therefore, the rainwater had difficulties to infiltrate into the slope and the factor of safety remained constant during 24 hours of rainfall.

In the JF slope, rainwater infiltrated into the slope slowly during 12 hours of rainfall causing the factor of safety to decrease gradually (Figure 13). Similar to the BT soil, the permeability of the JF soil was low due to the initially high matric suction of the JF slope. After 12 hours of rainfall, the matric suction of the JF soil had already decreased significantly and permeability of the soil also increased. Therefore, the factor of safety started to decrease at a faster rate and recovered gradually after reaching the minimum value of factor of safety. The minimum factor of safety was reached several hours after rainfall stopped regardless the intensity of rainfall. The JF slope with 9, 22 and 36 mm/hr rainfall reached the minimum factor of safety, one hour after the rainfall stopped. However, the JF slope with 80 mm/hr of rainfall reached the minimum factor of safety of 1.64, three hours after the rainfall stopped (Figure 13). The delay in reaching the minimum factor of safety occurred due to the low saturated permeability of the JF soil. At the end of the rainfall, rainwater had not reached the critical slip surface. It took some time for the rainwater to reach the critical point depending on the infiltration rate of the rainwater. The minimum factors of safety of the JF slope with an applied rainfall intensity of 22, 36 and 80 mm/hr were approximately similar. This indicated that a rainfall intensity of 22 mm/hr can be considered as a threshold value for residual soil slopes in Singapore.

Figure 12 shows that the factor of safety of the BT slope remained constant during a low intensity of rainfall (9 mm/hr) whereas the factor of safety of the JF slope (Figure 13) decreased quite significantly for the same rainfall intensity. This differing characteristic can be attributed to the permeability functions of the respective soils. Figure 8 shows that the permeability of the BT soil was lower at high suctions as compared to that of the JF soil. As a result, rain water infiltrated the BT slope at a slower rate than the infiltration rate in the JF slope, causing the factor of safety of the BT slope to remain essentially constant while the factor of safety of the JF slope decreased significantly.

4.5 Case Studies

Numerical analyses of two actual slopes located in the residual soils of the two main geological formations in Singapore were carried out using the actual slope geometry, soil properties and position of groundwater table and the results were compared with the finding from the parametric studies. The BT residual soil slope at Marsiling Road had a slope height (H) of 17 m and a slope angle of 27˚ (Figure 14). The first soil layer of the slope consisted of a silty sand with unit weight of 20 kN/m^3, effective cohesion of 9 kPa, effective angle of internal friction of 34˚, and ϕ^b angle of 21˚. The second soil layer consisted of a sandy silt with unit weight of 20 kN/m^3, effective cohesion of 0 kPa, effective angle of internal friction of 33˚, and ϕ^b angle of 26.1˚. The second slope selected for the case study was the JF residual soil slope at Jalan Kukoh with a slope height (H) of 12 m and slope angle of 33˚ (Figure 15). The slope consisted of two soil layers. The first layer was a clayey sand with unit weight of 20 kN/m^3, effective cohesion of 4 kPa, effective angle of internal friction of 33˚, and ϕ^b angle of 25˚. The second layer consisted of a clayey sand with unit weight of 20 kN/m^3, effective cohesion of 0 kPa, effective angle of internal friction of 36˚, and ϕ^b angle of 26.5˚.

Three piezometers were installed in the Marsiling Road slope to monitor the position of groundwater table with time. A 20 m long piezometer was placed at the crest of the slope (ℓ/L = 0), a 14 m long piezometer at mid-slope (ℓ/L = 0.33), and an 11 m long piezometer at the toe of the slope (ℓ/L = 0.93). The depths of groundwater table (h) were about 16.43 m, 10.85 m, and 4.74 m or (h/H = 0.96, 0.64, and 0.28) below the slope surface at the crest, mid, and toe of the slope, respectively. Figure 2 shows that the groundwater table of Marsiling Road slope was close to the groundwater table position for the BT soil at the driest period. Three piezometers were also installed in the Jalan Kukoh slope to observe the ground water table movement. Piezometers of 13, 10, and 6 m long were placed near the crest of the slope (ℓ/L = 0.15), at the mid-slope (ℓ/L = 0.25), and at the toe of the slope (ℓ/L = 1), respectively. The depths of groundwater table (h) were about 10 m, 10 m, and 3 m or (h/H = 0.83, 0.83, 0.25) below the slope surface near the crest, mid, and toe of the slope, respectively. Figure 3 shows that the groundwater table of Jalan Kukoh slope was close to the groundwater table position for the JF slope at the driest period.

SWCC for residual soils at Marsiling Road and Jalan Kukoh slopes are shown in Figures 16 and 17, respectively. The lines on the graph represent the best-fitted Fredlund and Xing SWCC equations whereas the symbols represent laboratory test results. In general, SWCC of the BT residual soil at Marsiling Road had a higher saturated volumetric water content, lower air-entry value, steeper slope, and lower residual water content than that of the JF residual soil at Jalan Kukoh. The measured saturated permeabilities of the first and second layers of the Marsiling Road residual soil were $6x10^{-6}$ m/s and $3.3x10^{-5}$ m/s, respectively. The saturated permeability of both clayey sand layers for Jalan Kukoh slope as obtained from laboratory test was $8.2x10^{-6}$ m/s. Figures 18 and 19 show the permeability functions of the residual soils at Marsiling Road and Jalan Kukoh slopes, respectively.

Seepage analyses of the slopes under 22 mm/hr rainfall intensity for 24 hr were performed using SEEP/W. Subsequently, slope stability analyses were conducted using SLOPE/W by importing the pore-water pressure distributions from SEEP/W seepage analyses. The comparison of factor of safety during 24 hours rainfall and after rainfall for the Marsiling Road and Jalan Kukoh slopes are shown in Figure 20.

Figure 20 shows that the initial factor of safety of the Marsiling Road slope (1.94) was higher than that of the Jalan Kukoh slope (1.79). The factor of safety of the Marsiling Road slope decreased rapidly during rainfall until it reached the minimum factor of safety of 1.54 at the end of rainfall. Similar behavior was also observed in the parametric studies of the BT residual soil slope under 22 mm/hr of rainfall. The high permeability of the soil allowed rainwater to infiltrate quickly and percolate down to greater depths of soil layers. This would result in a rapid increase in the pore-water pressures in the slope. Figure 20 also shows that the recovery rate of factor of safety for the Marsiling Road slope after rainfall was faster than that of the Jalan Kukoh slope due to the higher saturated permeability of the BT residual soil.

On the contrary, the factor of safety of the Jalan Kukoh slope decreased gradually to 1.43 after 24 hours of rainfall and continued to decline to the minimum factor of safety of 1.41 at 5 hours after the rainfall stopped. The lower saturated permeability of the JF slope caused a slower rainwater infiltration which delayed the occurrence of the minimum factor of

safety to some time later after the rainfall stopped. Similar behavior was also observed in the parametric studies for the JF slope under 22 mm/hr of rainfall.

The results from case studies show relatively good agreement with the results obtained from parametric studies for different positions of groundwater table. Case studies show that the factor of safety for the Marsiling Road slope at the driest period (1.94) decreased significantly during 12 hours of rainfall and continued to decrease gradually until it reached the minimum factor of safety (1.54) at the end of rainfall (Figure 20). The factor of safety for the Jalan Kukoh slope at the driest period (1.8) decreased gradually during 12 hours of rainfall and continued to decrease rapidly until reaching the minimum factor of safety (1.41) (Figure 20). This behavior was similar to those observed in the parametric studies for the BT and the JF slopes at the driest period (Figures 10 and 11, respectively). Although the minimum factor of safety obtained from the analyses did not indicate slope failures, other slope geometries or soil properties may produce a minimum factor of safety that corresponds to slope failure.

5 CONCLUSIONS

The groundwater table of residual soil slope from the sedimentary Jurong Formation (JF) has a larger variation between dry and wet periods as compared to the groundwater table of residual soil slope from the Bukit Timah Granite (BT) due to the large variation of soil types in residual soil slope from the sedimentary Jurong Formation.

At the driest period, the groundwater table of the JF slope is deeper than that of the BT slope. As a result, the factor of safety of the JF slope decreases more rapidly during rainfall as compared to that of the BT slope. At the wettest period, the groundwater table of slopes from both formations are located near the ground surface. As a result, the factors of safety of the JF and BT slopes decrease gradually during rainfall and also recover gradually after the rainfall stops.

The BT slope has coarser soil particles and higher permeability than the JF slope. As a result, the factor of safety of the BT slope decreases more rapidly than that of the JF slope under a rainfall intensity of 22, 36 and 80 mm/hr. The minimum factor of safety of the slope

from both formations will not change significantly if the applied rainfall intensity is higher than 22 mm/hr because the soil has reached its capacity to receive rainwater. However, the threshold rainfall intensity of 22 mm/hr still requires further investigation.

Soil properties affect the occurrence of the minimum factor of safety of slope. If a soil contains high percentage of fine particles, the air-entry value of the SWCC will be high, the permeability function will be gentle and the saturated permeability will be low. As a result, the minimum factor of safety may not occur at the end of rainfall, but several hours after the rainfall stops because rainwater has not reached the critical slip surface at the end of rainfall.

The variations in factor of safety from case studies showed similar trends with those obtained from parametric studies. However, different slope geometries and soil properties will result in different values of minimum factor of safety.

6 ACKNOWLEDGEMENTS

This work was supported by a research grant from a collaboration project between the Housing and Development Board and Nanyang Technological University (NTU), Singapore. The authors gratefully acknowledge the assistance of the Geotechnical Laboratory staff, School of Civil and Environmental Engineering, NTU, Singapore during the experiments and data collections.

7 REFERENCES

Agus, S.S., Leong, E.C. and Rahardjo, H. (2001). Soil-water Characteristic Curves of Singapore Residual Soils. *Journal of Geotechnical and Geological Engineering*. 19(3-4): 285–309.

Basile, A., Mele, G., and Terribile, F. (2003). Soil Hydraulic Behavior of A Selected Benchmark Soil Involved in The Landslide of Sarno 1998. *Geoderma*. 117(3-4): 331-346.

Brand, E.W. (1984). Landslides in Southeast Asia: A state-of-art report. *Proceedings of 13th International Conference on soil Mechanics and Foundation Engineering*, New Delhi, India. pp. 1013-1016.

Chatterjea, K. (1989). Observations on the Fluvial and Slope Processes in Singapore and their Impact on the Urban Environment, PhD Thesis, National University of Singapore.

Cho S.E. and Lee S.R. (2002). Evaluation of Surficial Stability for Homogeneous Slopes Considering Rainfall Characteristics. *Journal of Geotechnical and Geoenvironmental Engineering*, *ASCE*. 128(9): 756-763.

Fredlund, D.G. and Xing, A. (1994). Equations for the Soil-Water Characteristic Curve. *Canadian Geotechnical Journal*. 31: 533-546.

Fredlund, D.G. and Rahardjo, H. (1993). *Soil Mechanics for Unsaturated Soils*. John Wiley & Sons, Inc., New York.

Gasmo, J.M., Rahardjo, H. and Leong, E.C. (2000). Infiltration Effects on Stability of a Residual Soil Slope. *Computer and Geotechnics*. 26: 145–165.

Geoslope International Pte. Ltd. (2004a). *Seep /W for Finite Element Seepage Analysis*. Version 6.22: User's Guide, Geoslope International Ltd., Calgary, Alberta, Canada.

Geoslope International Pte. Ltd. (2004b). *Slope /W for Slope Stability Analysis*. Version 6.22: User's Guide, Geoslope International Ltd., Calgary, Alberta, Canada.

Kunze R. J., Uehara G. and Graham K. (1968). Factors important in the calculation of hydraulic conductivity. *Proc. of Soil Science Society America*. 32: 760-765.

Leong, E.C. and Rahardjo, H. (1997). A Review on Soil-Water Characteristic Curve Equations. *Journal of Geotechnical and Geoenvironmental Engineering, ASCE*. 123(12): 1106-1117.

Leong, E.C., Rahardjo, H., and Tang, S.K. (2002). Characterization and engineering properties of Singapore residual soils. *Proc. of the International Workshop on Characterization and Engineering Properties of Natural Soils*. pp. 1-10.

Lim, T.T., Rahardjo, H., Chang, M.F. and Fredlund, D.G. (1996). Effect of Rainfall on Matric Suction in a Residual Soil Slope. *Canadian Geotechnical Journal*. 33: 618-628.

Marshall, T. J. (1958). A relation between permeability and size distribution of pores. *Journal Soil Science*. 9: 1-8.

Millington, R. J. and Quirk, J. P. (1959). Permeability of porous media. *Nature*. 183: 387-388.

National Environment Agency (2007). *Meteorological Services Data*. National Environment Agency, Singapore.

Ng, C.W.W., Wang, B. and Tung, Y.K. (2001). Three-dimensional numerical investigations of groundwater responses in an unsaturated slope subjected to various rainfall patterns. *Canadian Geotechnical Journal*. 38: 1049−1062.

Ost, L., Van-Den, E.M., Poesen, J., and VAnmaercke-Gottigny, M.C. (2003). Characteristics and Spatial Distribution of Large Landslides in The Flemish Ardennes (Belgium). *Zeitschrift fur Geomorphologie N.F.* 47(3): 329-350.

Paulhus, J.L.H. (1965). Indian Ocean and Taiwan Rainfalls Set New Records. *Monthly Weather Review*. 93: pp. 331.

PUB (2000). *Code of Practice on Surface Water Drainage*. Public Utilities Board, Singapore.

PWD (1976). *Geology of the Republic of Singapore*. Public Works Department, Singapore.

Rahardjo, H., Leong, E.C. and Rezaur, R.B. (2008). Effect of Antecedent Rainfall on Pore-water Pressure Distribution Characteristics in Residual Soil Slopes under Tropical Rainfall. *Hydrological Processes*, Special Issue on Rainfall Induced Landslides and Debris Flow. 22: 506-523.

Rahardjo, H., Satyanaga, A., Leong, E.C., Ng, Y.S., Foo, M.D. and Wang, C.L. (2007). Slope Failures in Singapore due to Rainfall. *Proceedings of 10th Australia New Zealand Conference on Geomechanics "Common Ground"*. Brisbane, Australia. 2: 704-709.

Rahardjo, H., Ong, T.H., Rezaur, R.B. and Leong, E.C. (2007). Factors Controlling Instability of Homogeneous Soil Slopes under Rainfall Loading. *Journal of Geotechnical and Geoenvironmental Engineering, ASCE*. 133(12): 1532 – 1543.

Rahardjo, H., Lee, T.T., Leong, E.C. and Rezaur, R.B. (2005). Response of a Residual Soil Slope to Rainfall. *Canadian Geotechnical Journal*. 42(2): 340 – 351.

Rahardjo, H., Li, X.W., Toll, D.G. and Leong, E.C. (2001). The Effect of Antecedent Rainfall on Slope Stability. *Journal of Geotechnical and Geological Engineering*. Special Issue on "Unsaturated and Collapsible Soils." 19(3–4): 371 – 399.

Rahardjo H., Leong E.C., Deutcher M.S., Gasmo J.M., Tang, S.K. (2000). Rainfall-induced slope failures. *Geotechnical Engineering Monograph 3*. NTU-PWD Geotechnical Research Centre. Nanyang Technological University, Singapore. pp. 86.

Tan, S.B., Tan, S.L., Lim, T.L. and Yang, K.S. (1987). Landslides Problems and their control in Singapore. *Proceedings of 9th Southeast Asian Geotechnical Conference,* Bangkok. 1: 25-36.

Tohari A., Nishigaki M., and Komatsu M. (2007). Laboratory Rainfall-Induced Slope Failure with Moisture Content Measurement. *Journal of Geotechnical and Geoenvironmental Engineering*, *ASCE*. 133(5): 575-587.

Toll, D.G., H. Rahardjo and E.C. Leong (1999). Landslides in Singapore. *Proceedings of 2nd International Conference on Landslides, Slope Stability and the Safety of Infra-Structures*, Singapore. pp. 269-276.

Tsaparas, I., Rahardjo, H., Toll, D.G. and Leong, E.C. (2002). Controlling Parameters for Rainfall-Induced Landslides. *Computer and Geotechnics*. 29(1): 1-27.

List of Figures

Figure 1 Location of instrumented slopes in Singapore

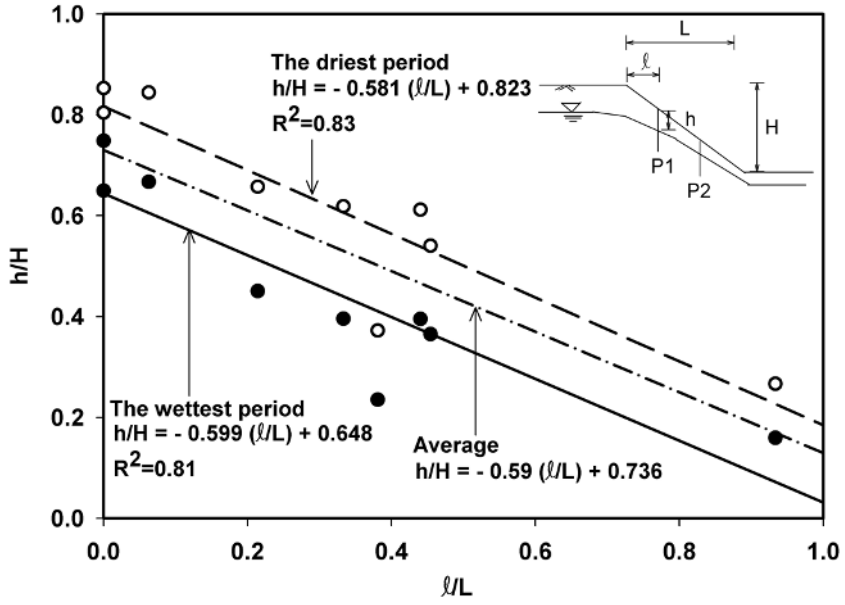

Figure 2 Variation of groundwater table position for the residual soil slopes from Bukit Timah Granite

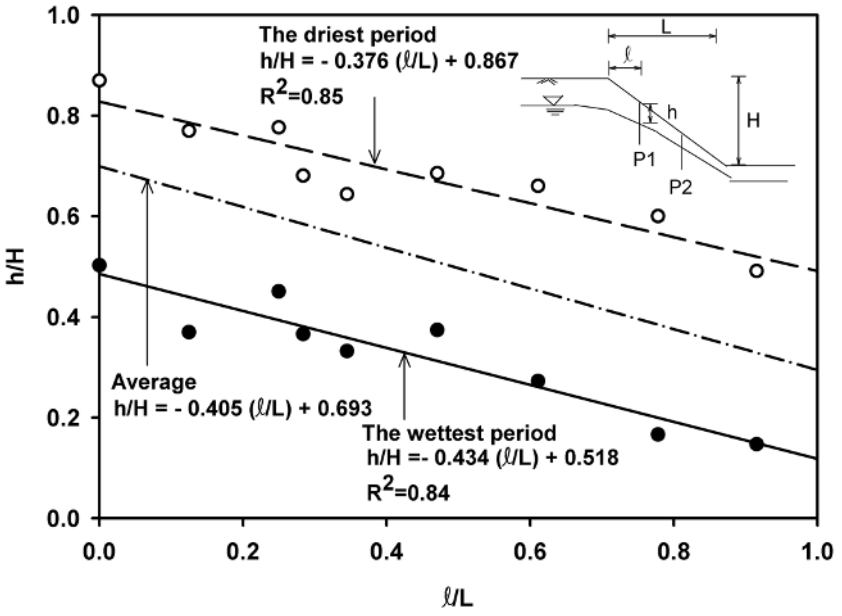

Figure 3 Variation of groundwater table position for the residual soil slopes from Jurong Formation

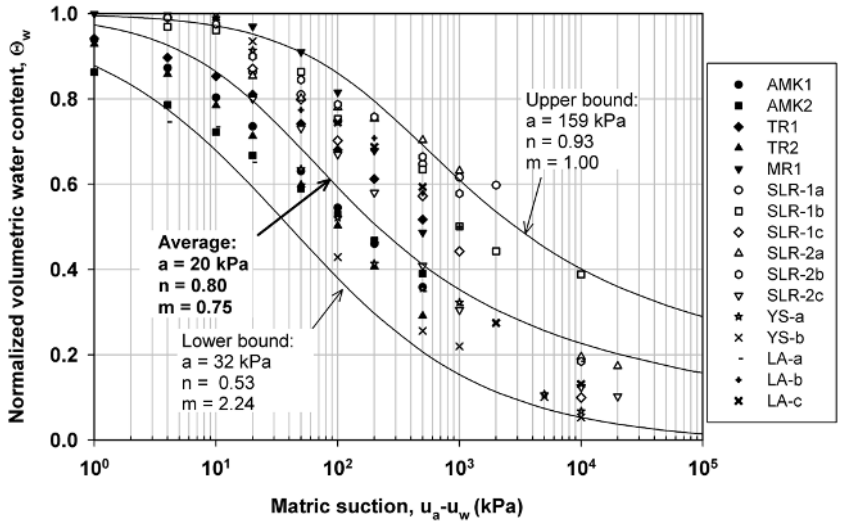

Figure 4 Normalized soil-water characteristic curves of the residual soils from Bukit Timah Granite (compiled data from Agus et al. (2001), AMK, TR, and MR observed slopes)

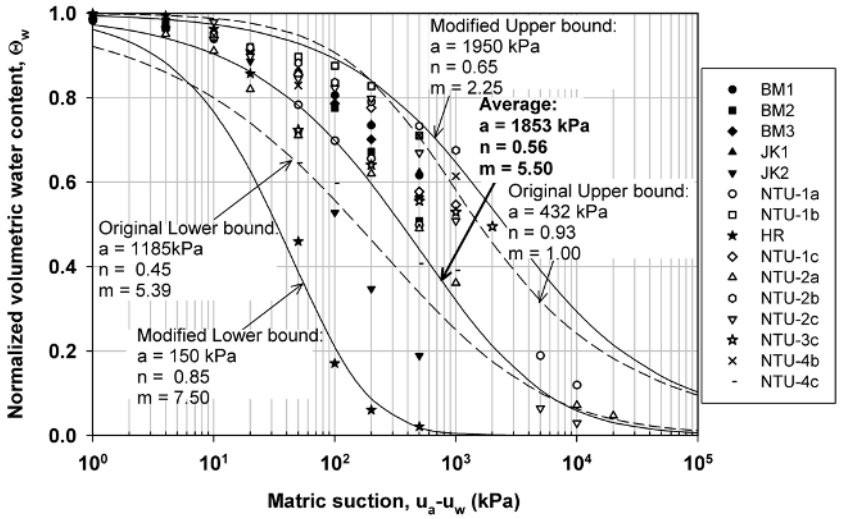

Figure 5 Normalized soil-water characteristic curves of the residual soils from Jurong Formation (compiled data from Agus et al. (2001), BM, JK, and HR observed slopes)

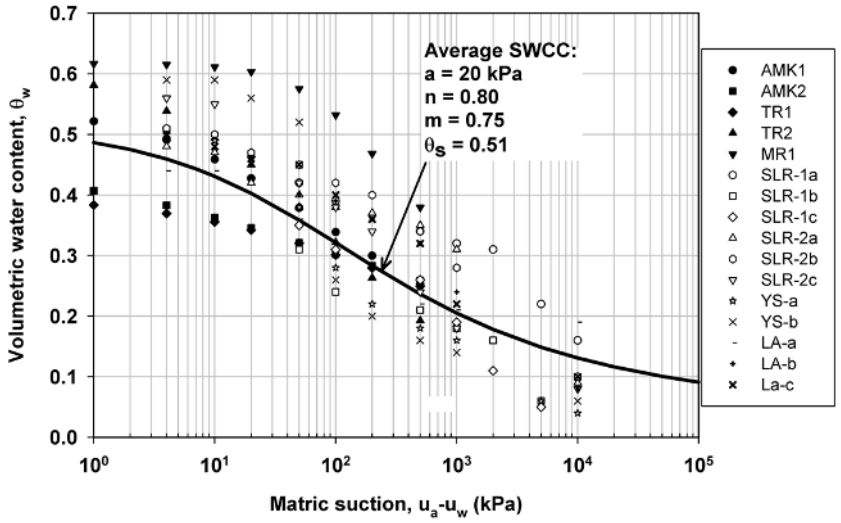

Figure 6 Soil-water characteristic curves of the residual soils from Bukit Timah Granite

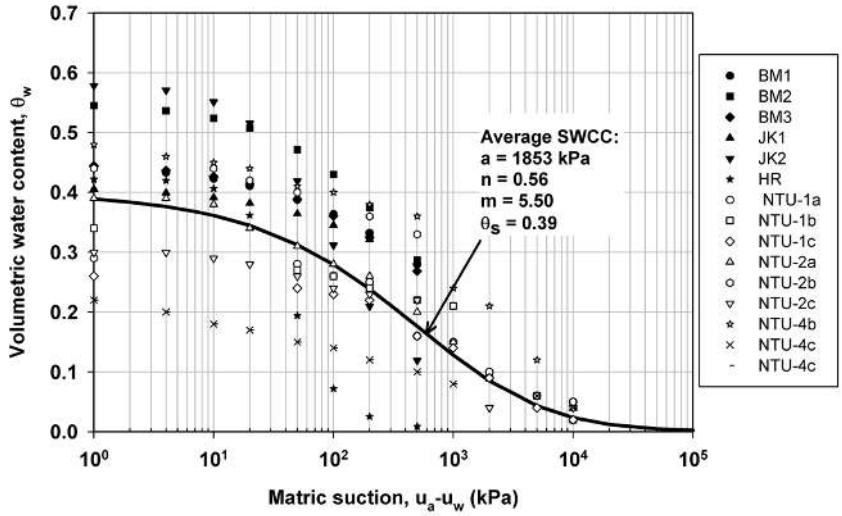

Figure 7 Soil-water characteristic curves of the residual soils from Jurong Formation

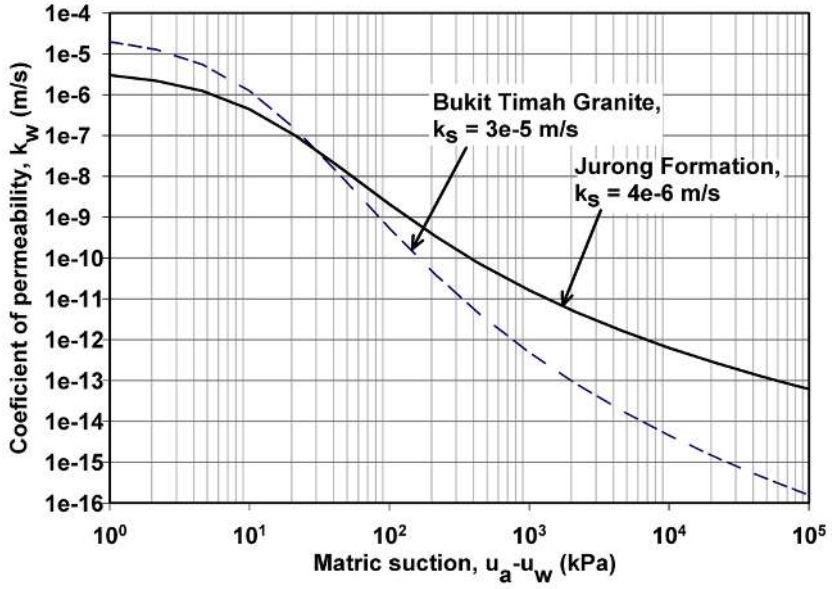

Figure 8 Permeability function of the residual soils from Bukit Timah Granite and Jurong Formation

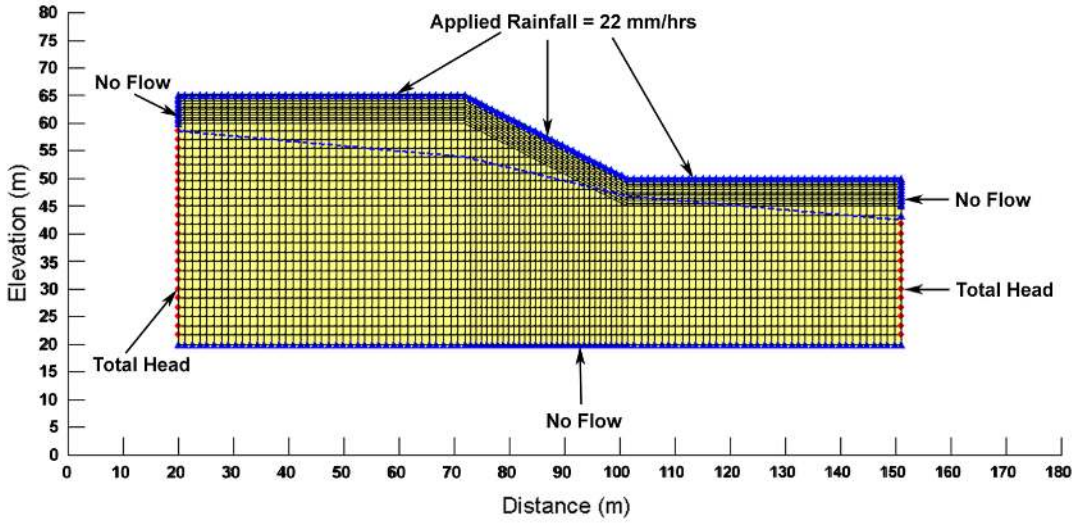

Figure 9 Slope model for parametric studies (slope height = 15 m and slope angle = 27°)

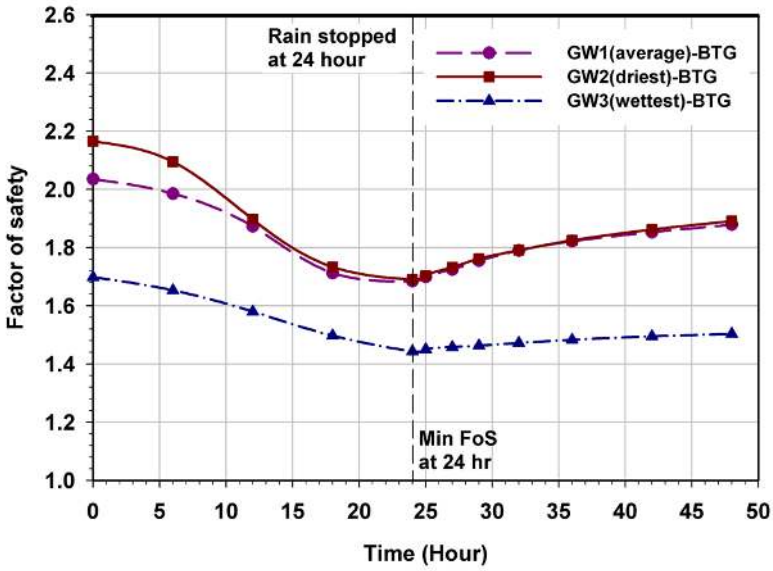

Figure 10 Variation of factor of safety of the slopes from Bukit Timah Granite for different groundwater table position (slope height = 15 m and slope angle = 27º)

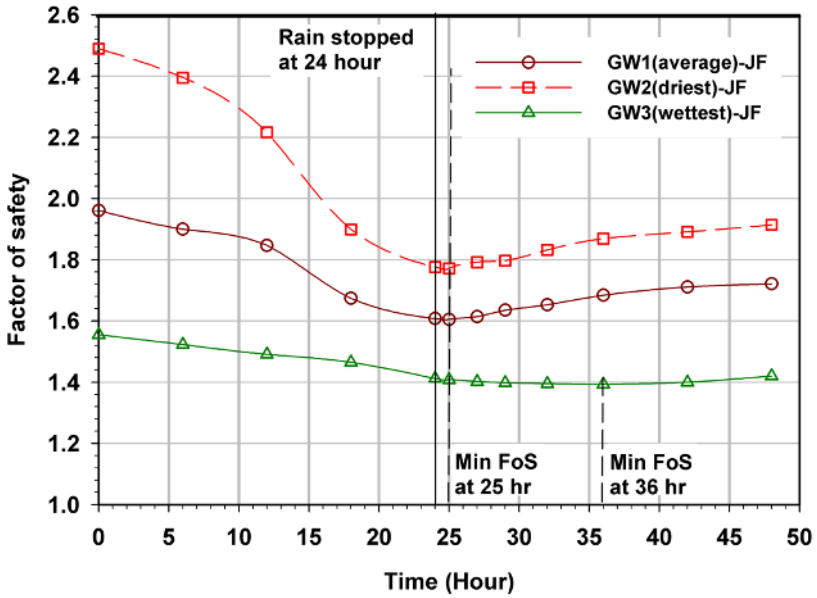

Figure 11 Variation of factor of safety of the slopes from Jurong Formation for different groundwater table position (slope height = 15 m and slope angle = 27º)

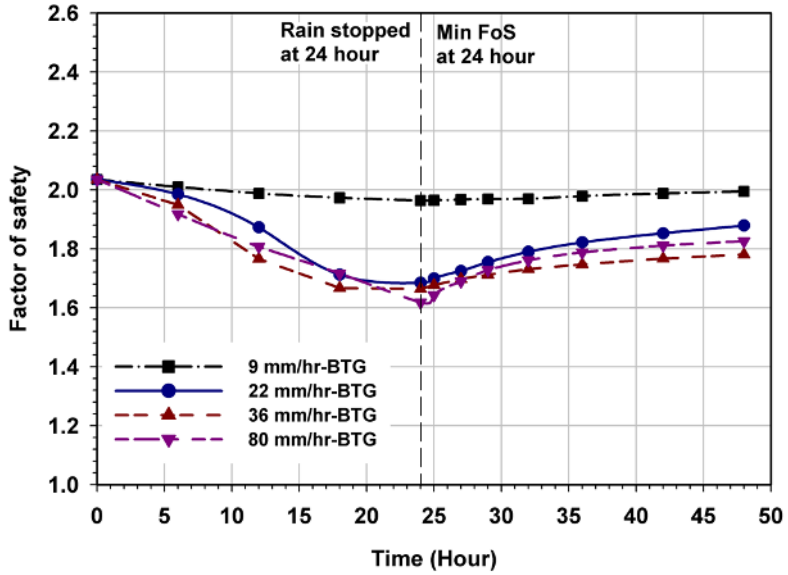

Figure 12 Variation of factor of safety of the slopes from Bukit Timah Granite for different rainfall intensities (slope height = 15 m and slope angle = 27º)

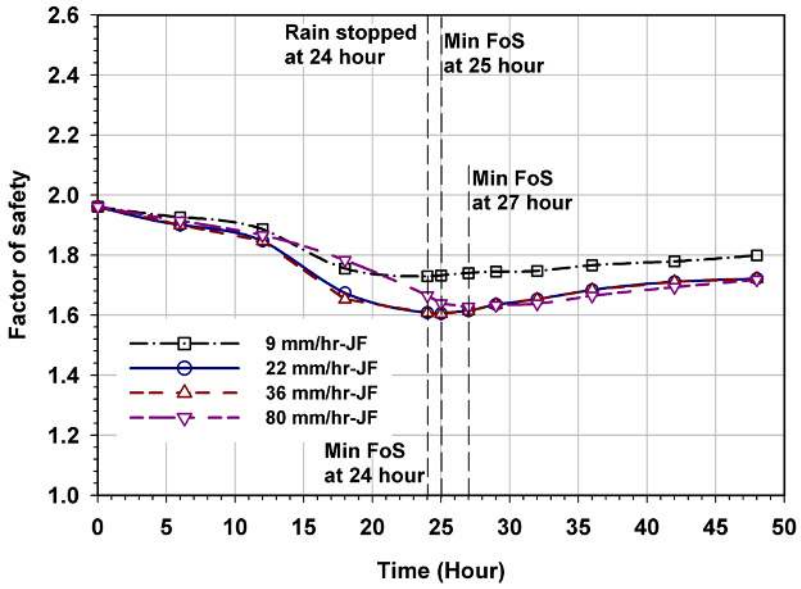

Figure 13 Variation of factor of safety of the slopes from Jurong Formation for different rainfall intensities (slope height = 15 m and slope angle = 27º)

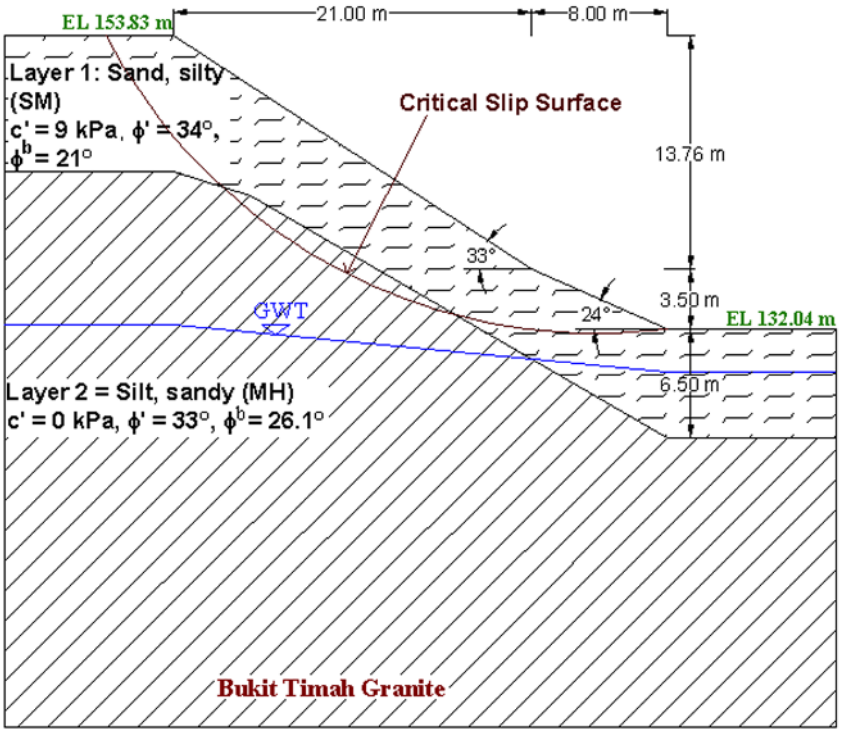

Figure 14 Soil profile of the slope from Bukit Timah Granite at Marsiling Road

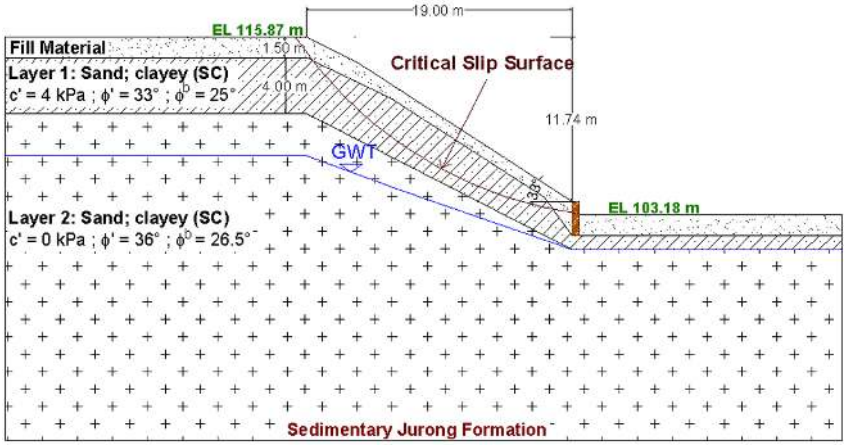

Figure 15 Soil profile of the slope from Jurong Formation at Jalan Kukoh

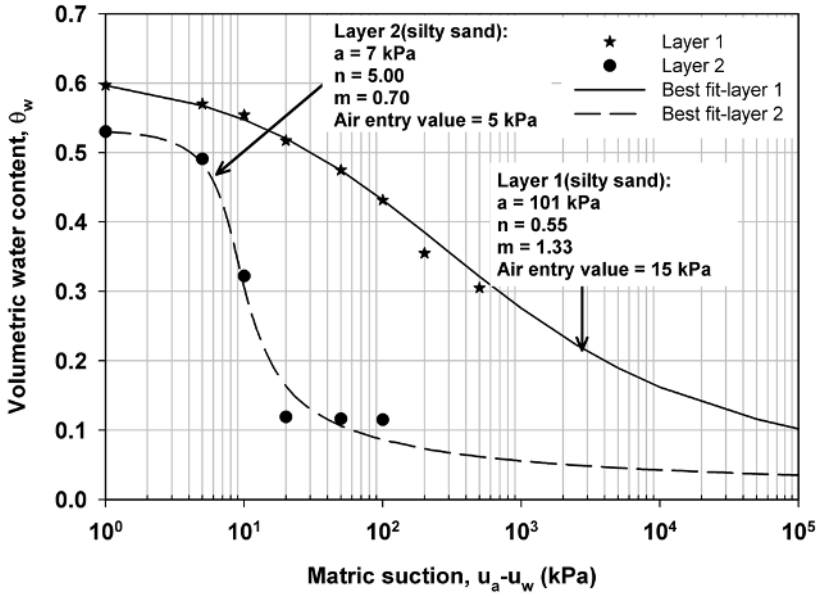

Figure 16 Soil-water characteristic curves of the residual soil from Bukit Timah Granite at Marsiling Road

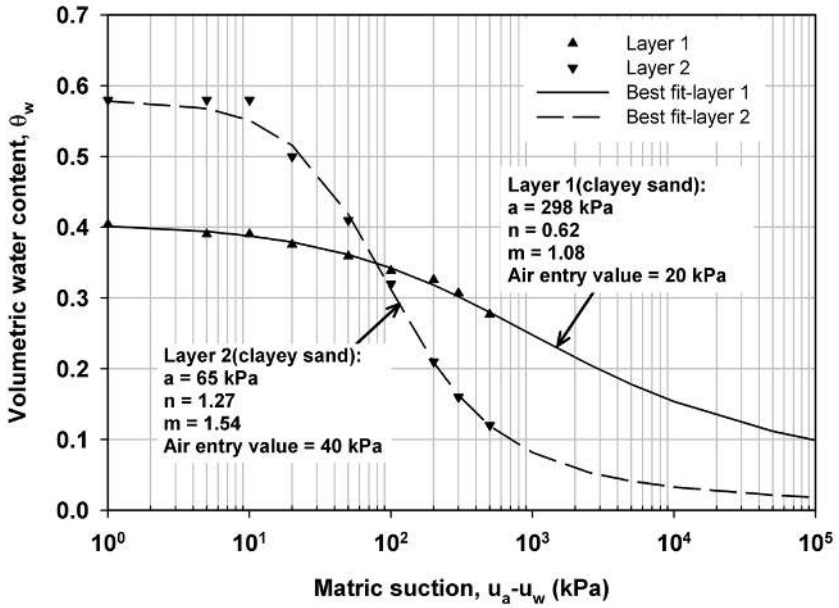

Figure 17 Soil-water characteristic curves of the residual soil from Jurong Formation at Jalan Kukoh

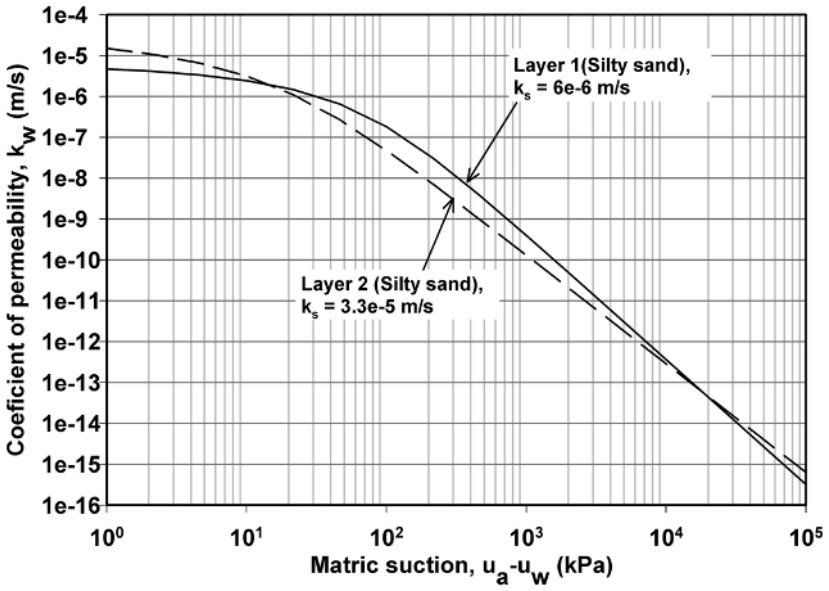

Figure 18 Permeability function of the residual soil from Bukit Timah Granite at Marsiling Road

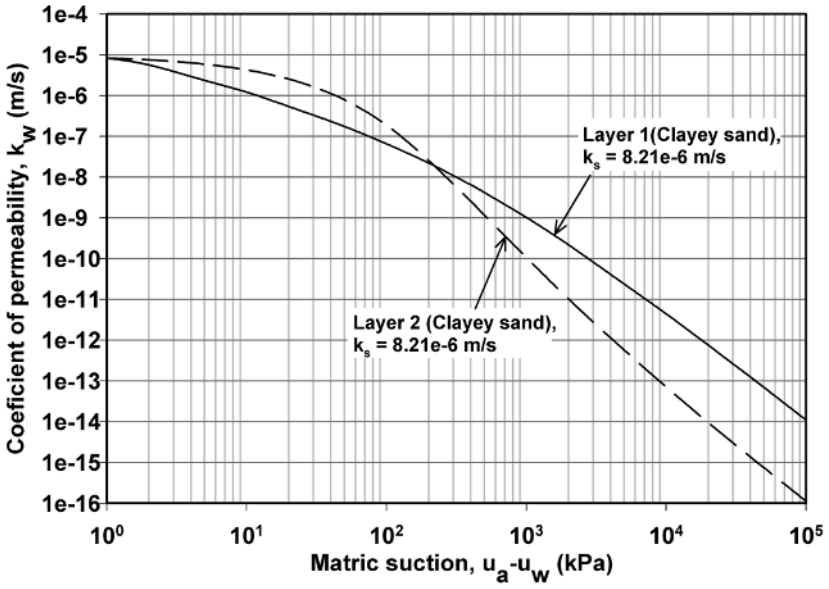

Figure 19 Permeability function of the residual soil from Jurong Formation at Jalan Kukoh

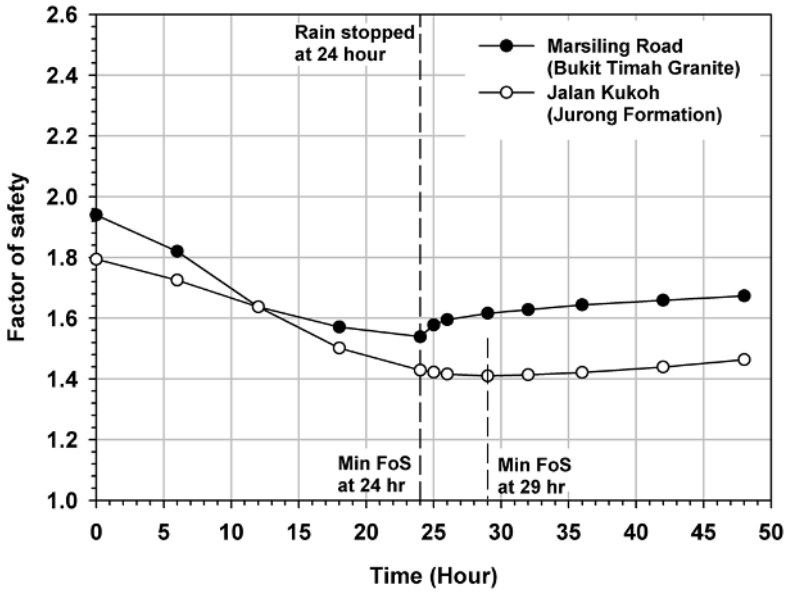

Figure 20 Factor of safety variation of residual soil slopes at Marsiling Road and Jalan Kukoh